Supplemental Materials

Molecular Biology of the Cell

Lacroix et al.

Supplemental Information for:

Lacroix et al. Identification of microtubule growth deceleration and its regulation by conserved and novel proteins

Supplemental Figures.

Figure S1

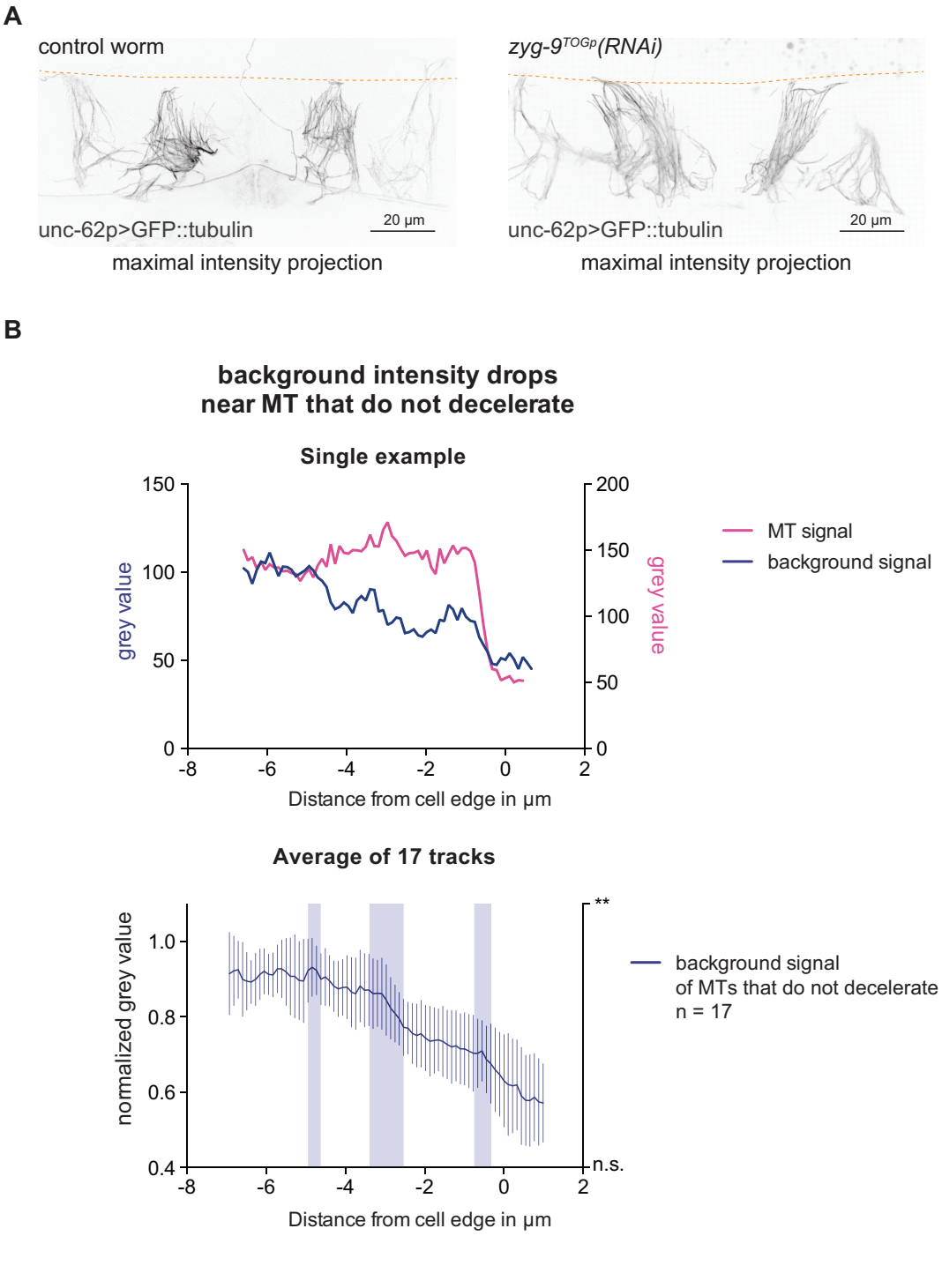

Figure S1: A drop in GFP-tubulin background intensity is observed in the vicinity of MTs that do not undergo growth deceleration. **(A)** Maximal intensity projections of 20 µm z-stacks on adult MDX12 worm in control situation of after 27h of ZYG-9^{TOGp} depletion by RNAi. GFP-tubulin under unc-62 promoter allows to visualize MT organization in uterine muscles which remains conserved after ZYG-9^{TOGp} depletion. **(B)** Top: example of intensity profile of a non-decelerating MT (pink trace) and its adjacent background (blue trace) both representing GFP-tubulin signal. Bottom: 17 individual background traces were normalized to their maximal intensity value and averaged and aligned relative to cell edge. As in Figure 3 (see also Experimental Procedures), for each x-axis position, the 4 pixels (0.88 µm) before and after each position were compared by t-test to evaluate whether there was a significant drop in intensity. The vertical shaded bars represent pixels for which the difference was significant (** = $P \leq 0.01$, plotted on right y-axis). Error bars = 95% confidence interval.

Figure S2

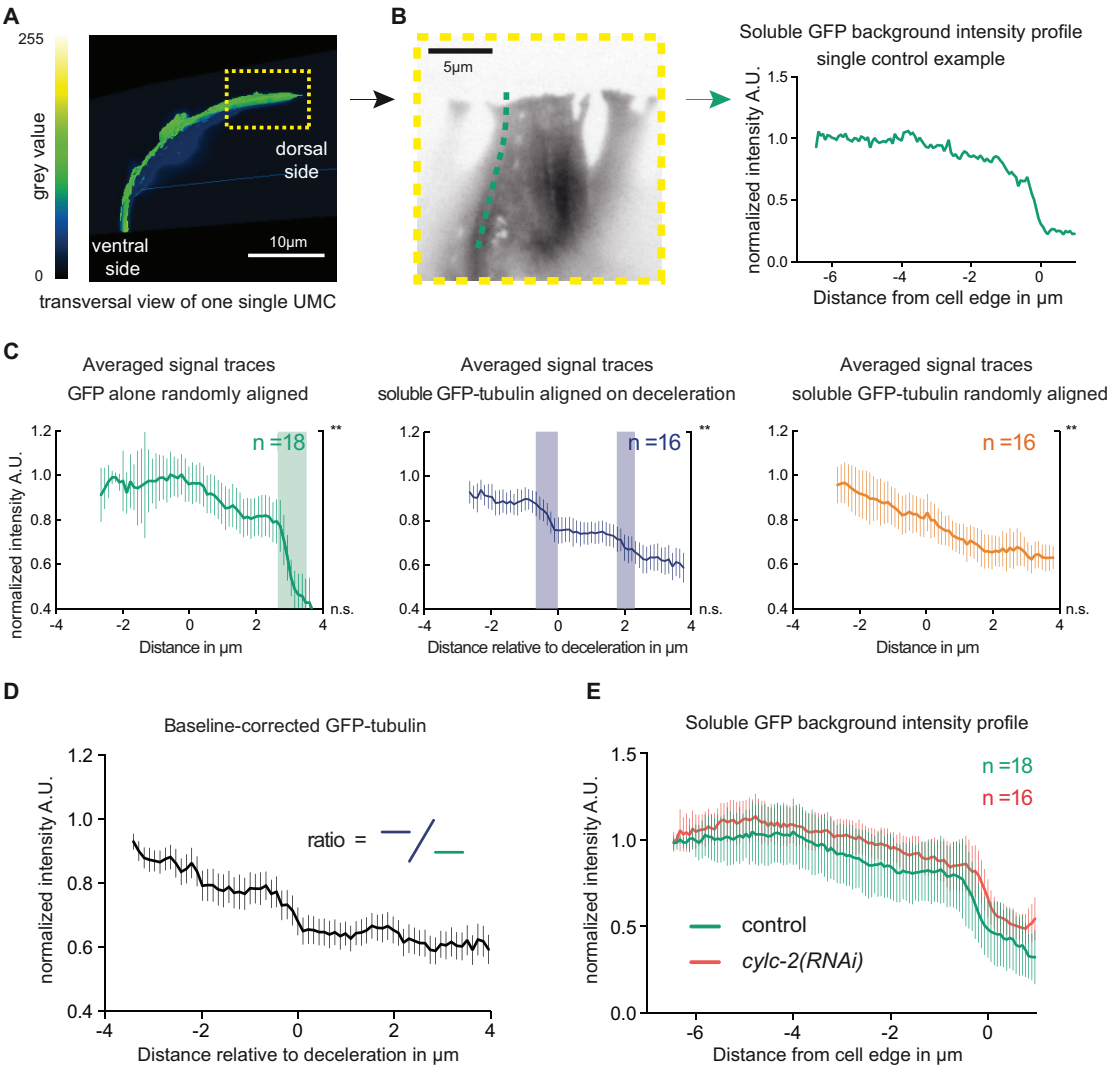
A
255
grey value
0
dorsal side
ventral side
10µm
transversal view of one single UMC
B
5µm
Soluble GFP background intensity profile
single control example
normalized intensity A.U.
Distance from cell edge in µm
C
Averaged signal traces
GFP alone randomly aligned
n =18
normalized intensity A.U.
Distance in µm
Averaged signal traces
soluble GFP-tubulin aligned on deceleration
n =16
Distance relative to deceleration in µm
Averaged signal traces
soluble GFP-tubulin randomly aligned
n =16
Distance in µm
n.s.
**
D
Baseline-corrected GFP-tubulin
ratio =
normalized intensity A.U.
Distance relative to deceleration in µm
E
Soluble GFP background intensity profile
n =18
n =16
control
cylc-2(RNAi)
normalized intensity A.U.
Distance from cell edge in µm

Figure S2: CYLC-2 depletion does not affect GFP distribution in UMCs. **(A)** Soluble GFP expressed in UMCs is used to reveal the cell topology and the organization of non-tubulin protein content. Transversal view of a 3D volume reconstruction pseudo-color made with Imaris software of an UMC expressing GFP under *unc-62* promoter. The image shows the continuously flat dorsal extension (yellow dashed rectangle represent the dorsal extension where deceleration occurs). **(B)** Single confocal plane of a UMC dorsal extension expressing soluble GFP and the measured GFP intensity of a single track along the UMC ventral-to-dorsal axis, as represented by the dotted green line. No obvious drop was detected, but intensity progressively reduced approaching the cell edge. **(C)** Green line represents the average intensity of several GFP alone tracks (as in B). Blue line corresponds to the average soluble GFP-tubulin signal of tracks (as main Figure 3) next to a decelerating MT in UMC. Blue traces were aligned on the deceleration point of the juxtaposed MT before being averaged. To generate the orange line, the same traces as in blue were aligned on a random point instead of the deceleration point. Since green and orange traces were randomly aligned, and because UMC dimensions are really constant, curves were arbitrarily positioned on the x-axis based on the expected position of deceleration relative to cell edge. The drop is not visible when traces are aligned on a random position and averaged (orange curve). As in Figure 3 and S1, for each x-axis position, the 4 pixels (0.88 µm) before and after each position were compared by t-test to evaluate whether there was a significant drop in intensity. The vertical shaded bars represent pixels for which the difference was significant (** = $P \leq 0.01$). **(D)** Ratio of soluble GFP-tubulin signal over GFP alone aligned on cell edge, the decay in GFP-tubulin is seen also on this "baseline-corrected" curve indicating that the decay is not simply due to a decay in global fluorescence intensity of any protein. **(E)** Average intensity profile of control (green) and CYLC-2 depleted cells (red) cell expressing soluble GFP. **(B to D)** all signals were normalized on the average of the first 7 pixels of the track as reference in order to minimize variation due to noise. Error bars = 95% confidence interval.

Figure S3

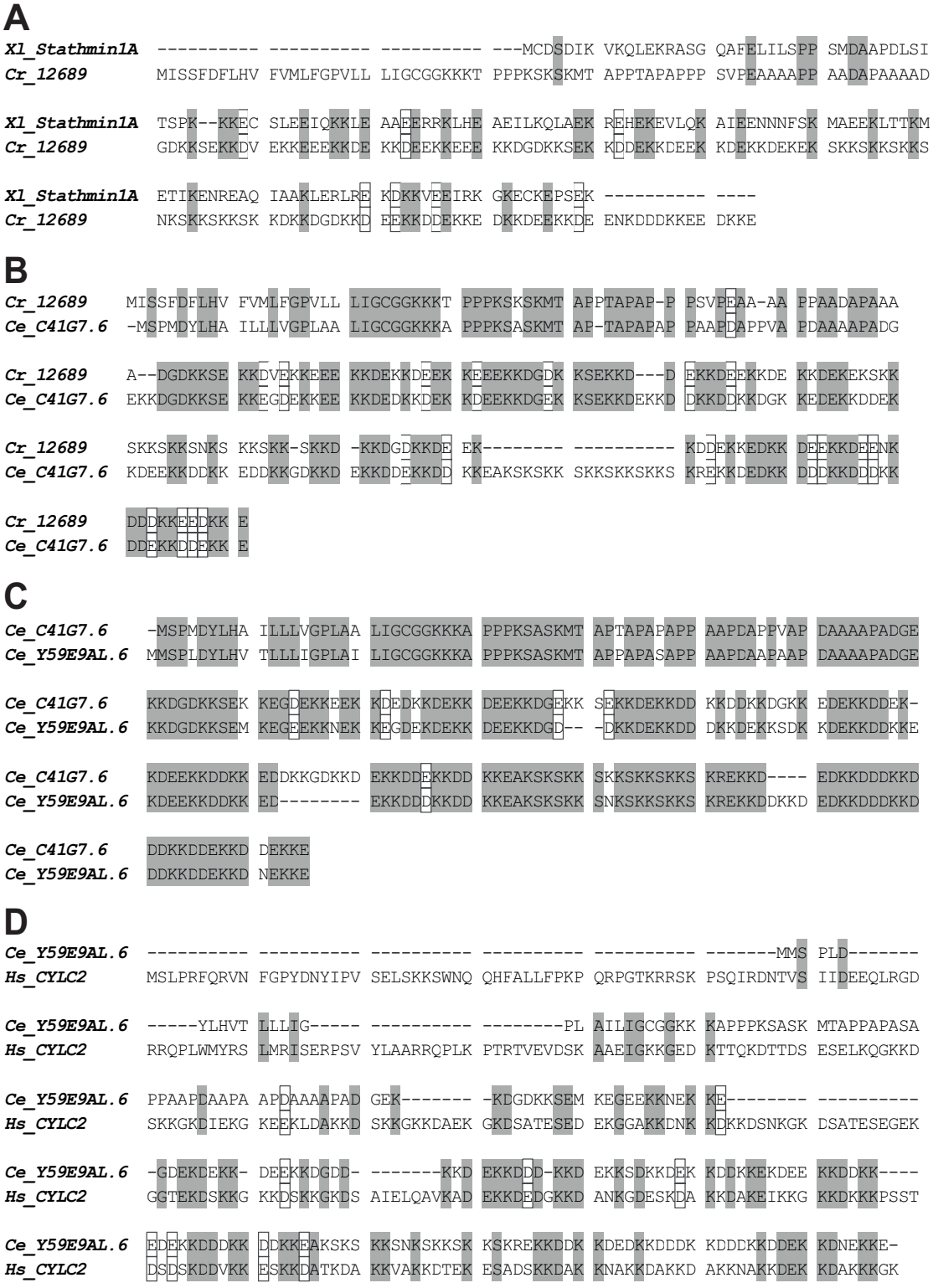
A
Xl_Stathmin1A ---------- ---------- ---------- ---MCDSDIK VKQLEKRASG QAFELILSPP SMDAAPDLSI
Cr_12689 MISSFDFLHV FVMLFGPVLL LIGCGGKKKT PPPKSKSKMT APPTAPAPPP SVPEAAAAPP AADAPAAAAD
Xl_Stathmin1A TSPK--KKEC SLEEIQKKLE AAEERRKLHE AEILKQLAEK REHEKEVLQK AIEENNNFSK MAEEKLTTKM
Cr_12689 GDKKSEKKDV EKKEEEKKDE KKDEEKKEEE KKDGDKKSEK KDDEKKDEEK KDEKKDEKEK SKKSKKSKKS
Xl_Stathmin1A ETIKENREAQ IAAKLERLRE KDKKVEEIRK GKECKEPSEK ---------- ----
Cr_12689 NKSKKSKKSK KDKKDGDKKD EEKKDDEKKE DKKDEEKKDE ENKDDDKKEE DKKE
B
Cr_12689 MISSFDFLHV FVMLFGPVLL LIGCGGKKKT PPPKSKSKMT APPTAPAP-P PSVPEAA-AA PPAADAPAAA
Ce_C41G7.6 -MSPMDYLHA ILLLVGPLAA LIGCGGKKKA PPPKSASKMT AP-TAPAPAP PAAPDAPPVA PDAAAAPADG
Cr_12689 A--DGDKKSE KKDVEKKEEE KKDEKKDEEK KEEEKKDGDK KSEKKD---D EKKDEEKKDE KKDEKEKSKK
Ce_C41G7.6 EKKDGDKKSE KKEGDEKKEE KKDEDKKDEK KDEEKKDGEK KSEKKDEKKD DKKDDKKDGK KEDEKKDDEK
Cr_12689 SKKSKKSNKS KKSKK-SKKD -KKDGDKKDE EK-------- ---------- KDDEKKEDKK DEEKKDEENK
Ce_C41G7.6 KDEEKKDDKK EDDKKGDKKD EKKDDEKKDD KKEAKSKSKK SKKSKKSKKS KREKKDEDKK DDDKKDDDKK
Cr_12689 DDDKKEEDKK E
Ce_C41G7.6 DDEKKDDEKK E
C
Ce_C41G7.6 -MSPMDYLHA ILLLVGPLAA LIGCGGKKKA PPPKSASKMT APTAPAPAPP AAPDAPPVAP DAAAAPADGE
Ce_Y59E9AL.6 MMSPLDYLHV TLLLIGPLAI LIGCGGKKKA PPPKSASKMT APPAPASAPP AAPDAAPAAP DAAAAPADGE
Ce_C41G7.6 KKDGDKKSEK KEGDEKKEEK KDEDKKDEKK DEEKKDGEKK SEKKDEKKDD KKDDKKDGKK EDEKKDDEK-
Ce_Y59E9AL.6 KKDGDKKSEM KEGDEKKNEK KEGDEKDEKK DEEKKDGD-- -DKKDEKKDD DKKDEKKSDK KDEKKDDKKE
Ce_C41G7.6 KDEEKKDDKK EDDKKGDKKD EKKDDEKKDD KKEAKSKSKK SKKSKKSKKS KREKKD---- EDKKDDDKKD
Ce_Y59E9AL.6 KDEEKKDDKK ED-------- EKKDDDKKDD KKEAKSKSKK SNKSKKSKKS KREKKDDKKD EDKKDDDKKD
Ce_C41G7.6 DDKKDDEKKD DEKKE
Ce_Y59E9AL.6 DDKKDDEKKD NEKKE
D
Ce_Y59E9AL.6 ---------- ---------- ---------- ---------- ---------- -------MMS PLD-------
Hs_CYLC2 MSLPRFQRVN FGPYDNYIPV SELSKKSWNQ QHFALLFPKP QRPGTKRRSK PSQIRDNTVS IIDEEQLRGD
Ce_Y59E9AL.6 -----YLHVT LLLIG----- ---------- --------PL AILIGCGGKK KAPPPKSASK MTAPPAPASA
Hs_CYLC2 RRQPLWMYRS LMRISERPSV YLAARRQPLK PTRTVEVDSK AAEIGKKGED KTTQKDTTDS ESELKQGKKD
Ce_Y59E9AL.6 PPAAPDAAPA APDAAAAPAD GEK------- -KDGDKKSEM KEGEEKKNEK KE-------- ----------
Hs_CYLC2 SKKGKDIEKG KEEKLDAKKD SKKGKKDAEK GKDSATESED EKGGAKKDNK KDKKDSNKGK DSATESEGEK
Ce_Y59E9AL.6 -GDEKDEKK- DEEKKDGDD- -------KKD EKKDDD-KKD EKKSDKKDEK KDDKKEKDEE KKDDKK----
Hs_CYLC2 GGTEKDSKKG KKDSKKGKDS AIELQAVKAD EKKDEDGKKD ANKGDESKDA KKDAKEIKKG KKDKKKPSST
Ce_Y59E9AL.6 EDEKKDDDKK DDKKEAKSKS KKSNKSKKSK KSKREKKDDK KDEDKKDDDK KDDDKKDDEK KDNEKKE-
Hs_CYLC2 DSDSKDDVKK ESKKDATKDA KKVAKKDTEK ESADSKKDAK KNAKKDAKKD AKKNAKKDEK KDAKKKGK

Figure S3: Sequence alignments of CYLC-1 and CYLC-2 ORFs with their homologues. The *C. elegans* genome contains genes with homology to stathmins and cylicin. Genes encoding stathmin had not been annotated in the *C. elegans* genome (Cassimeris, 2002). Using stathmin sequence from *Xenopus laevis* (gene name stmn1-a), the NCBI tools (PSI-BLAST and/or PHI-BLAST) were used to identify to find sequence, domain or pattern homology in nematodes genomes. Among these searches we identified *Caenorhabditis remanei* uncharacterized protein CRE12689 (NCBI sequence XP_003108008.1). Wormbase BLAST search tools were used to search for similarity within the *Caenorhabditis elegans* genome. Alignments created with ClustalW algorithm (EMBL-EBI) are shown. (A) The *Xenopus laevis* stathmin-1-A is aligned with the *C. remanei* protein CRE12689. (B) The CRE12689 is aligned with the C41G7.6 protein identified in the *C. elegans* genome. (C) The two *C. elegans* proteins C41G7.6 and its close homologue Y59E9AL.6 are aligned. Y59E9AL.6 and C41G7.6, were named CYLC-1 and CYLC-2, respectively, based on their relative homology to human protein cylicin. (D) The *C. elegans* ORF Y59E9AL.6 is annotated in Wormbase as a homologue of the human protein Cylicin-2. (A, B, C and D) Identical bases are shaded; positions with negatively charged residues E or D in both sequences are framed.

Figure S4

$$J = \frac{R_{grow} \cdot f_{rescue} - R_{shrink} \cdot f_{cat}}{f_{cat} + f_{rescue}}$$

$J > 0$ = unbounded state

$J < 0$ = bounded state

	UMC global	dorsal	inter.	soma
Growth rate	0.15	0.11	0.18	0.19
Shrinkage rate	0.85	0.82	0.87	0.93
Catastrophe frequency	0.045	0.14	0.06	0.07
Rescue frequency	0.28	0.55	0.35	0.38
	$J > 0$	$J < 0$	$J > 0$	$J > 0$

Figure S4: Prediction of the boundary state in UMCs and their subcellular regions. The equation devised by Leibler and colleagues calculates the average velocity of the growth of the MT population: *J* (Verde et al., 1992). This value is calculated using the four dynamics parameters: R_{grow} (growth rate), R_{shrink} (shrinkage rate), f_{cata} (catastrophe frequency) and f_{rescue} (rescue frequency). The table contains the parameters of MT dynamics from this study for UMCs and the 3 different subcellular regions: dorsal extension, intermediate and soma. Globally, measured dynamic instability parameters predict that MTs are in the unbounded state in UMCs, except in the dorsal extension.

Figure S5

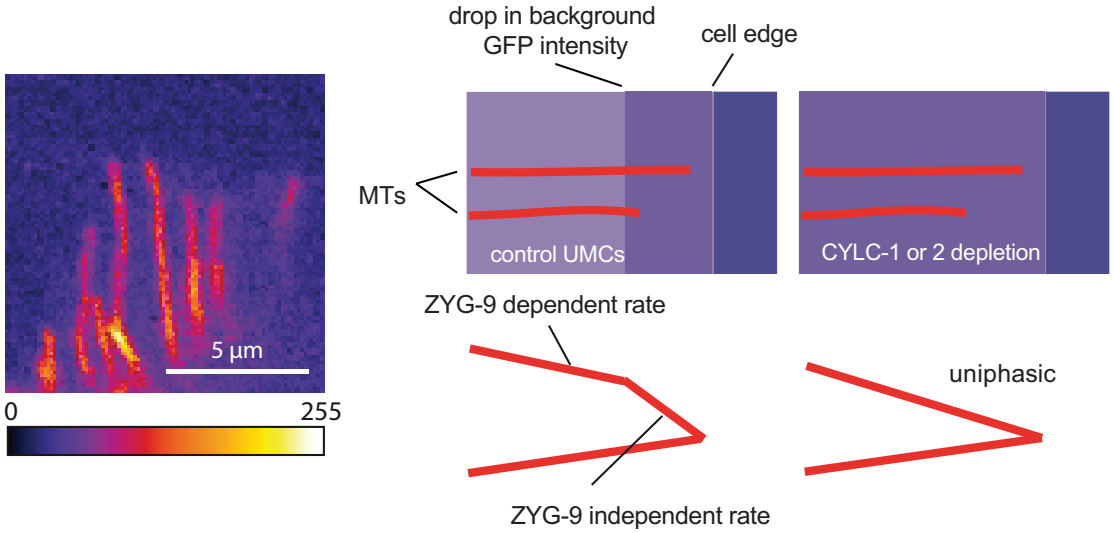

Figure S5: Model of MT deceleration regulation. Our results suggest that CYLC-1 and CYLC-2 promote soluble tubulin compartmentalization in UMCs cytoplasm with a reduced tubulin concentration at the dorsal cell extension and/or regulate ZYG-9 activity in the dorsal extension. The compartmentalization allows two distinct behaviors to be adopted by a single MT. First, ZYG-9^{TOGp} mediates rapid, persistent growth excursions; second, MTs exhibit a slower growth phase when reaching the periphery of the dorsal extension. In this region, MTs also display distinct dynamics, including higher rescue and catastrophe frequencies, in addition to reduced growth rate.

Supplemental Tables

Tables S1

population	A			B			C		
	mean	sem	n	mean	sem	n	mean	sem	n
Growth rate (µm/sec)	0.11	0.01	63	0.18	0.01	31	0.19	0.01	35
Growth length (µm)	0.75	0.05	63	2.79	0.22	31	2.62	0.20	35
Growth duration (sec)	6.96	0.34	63	16.76	1.89	31	14.21	1.13	35
Shrinking rate (µm/sec)	0.82	0.06	48	0.87	0.05	33	0.93	0.04	33
Shrinking length (µm)	1.33	0.15	48	2.33	0.17	33	2.38	0.22	33
Shrinking duration (sec)	1.83	0.25	48	2.85	0.22	33	2.64	0.24	33
Catastrophe (sec-1)	0.14	0.01	63	0.06	0.01	31	0.07	0.01	35
Catastrophe (µm-1)	1.34	0.09	63	0.36	0.03	31	0.38	0.03	35
Rescue (sec-1)	0.55	0.07	48	0.35	0.03	33	0.38	0.03	33
Rescue (µm-1)	0.75	0.09	48	0.43	0.03	33	0.42	0.04	33

Table S1: Dynamic parameters of MTs in different topological subcellular compartment called region A (At the cell edge), B (before the cell edge) and C (C center). The region A corresponds to the last 2 µm before the UMC-seam cells contact on the dorsal cellular extension of UMCs. n: number of MTs per condition. n(worms) ≥ 12.

Tables S2

population	initial			terminal			total		
	mean	sem	n	mean	sem	n	mean	sem	n
Growth rate (µm/sec)	0.22	0.01	98	0.10	0.002	69	0.15	0.003	169
Growth length (µm)	3.23	0.10	98	1.24	0.02	69	3.21	0.08	169
Growth duration (sec)	15.67	0.55	98	13.92	0.41	69	22.34	0.56	169
Shrinking rate (µm/sec)	0.89	0.03	98	0.72	0.03	69	0.85	0.02	169
Catastrophe (sec-1)	0.06	0.002	98	0.07	0.002	69	0.04	0.001	169
Rescue (sec-1)	0.21	0.01	98	0.51	0.03	69	0.28	0.01	169

Table S2: Dynamic parameters of initial and terminal phases of biphasic MTs are compared to the total MT population in UMCs. n: number of MTs per condition. n(worms) ≥ 10.

Tables S3

	control			control (terminal)			*cylc-1(RNAi)*			*cylc-2(RNAi*			*zyg-9(RNAi)*		
Dynamic parameters	mean	SEM	n	mean	SEM	n	mean	SEM	n	mean	SEM	n	mean	SEM	n
Growth rate	0,18	0,003	199	0,11	0,002	265	0,18	0,005	182	0,13	0,003	312	0,09	0,002	298
Growth length	2,25	0,11	198	0,60	0,02	265	3,22	0,15	182	2,85	0,12	312	1,19	0,06	298
Growth duration	12,36	0,57	198	5,53	0,17	265	19,13	0,89	182	24,40	1,10	312	12,68	0,58	298
Shrinkage rate	0,80	0,03	139	0,82	0,03	139	0,66	0,02	222	0,71	0,02	340	0,57	0,02	156
Shrinkage length	2,88	0,19	139	1,17	0,05	139	3,91	0,26	222	4,02	0,22	340	2,40	0,11	156
Shrinkage duration	3,83	0,27	139	1,53	0,07	139	2,53	0,16	222	2,63	0,14	340	4,75	0,26	156
Catastrophe frequency	0,08	0,004	199	0,18	0,01	265	0,05	0,002	182	0,04	0,002	312	0,08	0,004	298
Rescue frequency	0,26	0,02	139	0,65	0,03	139	0,26	0,02	222	0,25	0,01	340	0,21	0,01	156

Table S3: Effect of CYLC-1, CYLC-2 and ZYG-9^{TOGp} depletions on MT dynamics in UMCs of adult worms. Units are *µm/sec* for rates, *µm* for lengths, *seconds* for durations and *seconds*$^{-1}$ for frequencies. n: number of MTs per condition. n(worms) ≥ 12.

Supplemental References

Cassimeris, L. 2002. The oncoprotein 18/stathmin family of microtubule destabilizers. *Curr Opin Cell Biol*. 14:18-24.

Verde, F., M. Dogterom, E. Stelzer, E. Karsenti, and S. Leibler. 1992. Control of microtubule dynamics and length by cyclin A- and cyclin B-dependent kinases in Xenopus egg extracts. *J Cell Biol*. 118:1097-1108.